Bamfordite, Fe³⁺Mo₂O₆(OH)₃·H₂O, a new hydrated iron molybdenum oxyhydroxide from Queensland, Australia: Description and crystal chemistry

WILLIAM D. BIRCH,[1] ALLAN PRING,[2] E. MAUDE MCBRIAR,[2] BRYAN M. GATEHOUSE,[3] AND
CATHERINE A. MCCAMMON[4]

[1]Department of Mineralogy, Museum of Victoria, 328 Swanston Street, Melbourne, 3000, Victoria, Australia
[2]Department of Mineralogy, South Australian Museum, North Terrace, Adelaide, 5000, South Australia
[3]Department of Chemistry, Monash University, Clayton, 3168, Victoria, Australia
[4]Bayerisches Geoinstutit, Universität Bayreuth, 95440 Bayreuth, Germany

ABSTRACT

Bamfordite from the abandoned W-Mo-Bi mines at Bamford, Queensland, Australia, is a new hydrated iron molybdate with a unique structure. This mineral formed by oxidation of molybdenite, MoS_2, in the presence of strongly acidic solutions. It occurs as microcrystalline aggregates of tabular triclinic crystals between 0.005 and 0.05 mm long. The aggregates are apple-green with an earthy luster and greenish yellow streak. Crystals are transparent, with pale to moderate yellow-green pleochroism. They show principal forms $\{001\}$, $\{100\}$, $\{010\}$, $\{110\}$, $\{1\bar{1}0\}$, and prominent (100) cleavage traces. The Mohs hardness is 2–3 and the measured density is 3.620 g/cm³ (calculated density is 3.616 g/cm³). Crystals are biaxial negative and length slow, with RIs of α = 1.91, β = 2.03, and γ = 2.11, and $2V \approx 90°$. Chemical analysis yielded an empirical formula of $Fe^{3+}_{1.00}$ $Mo_{2.01}W_{0.03}$ $P_{0.02}O_{10}H_{4.62}$, calculated on the basis of ten O atoms. The simplified formula is $Fe^{3+}Mo_2O_6$ $(OH)_3 \cdot H_2O$, chosen on the basis of crystal-structure determination and Mössbauer spectroscopy results. Unit-cell parameters calculated both from the X-ray powder and single-crystal diffraction data are a = 5.889(5), b = 7.545(5), c = 9.419(5) Å; α = 71.46(4)°, β = 83.42(4)°, γ = 72.78(4)°; V = 378.9(4) Å³; Z = 2; $P1$ or $P\bar{1}$. The crystal structure was solved in $P1$ using direct methods and Fourier techniques. The final refinement based on 1486 observed reflections $[I > 2.00\ \sigma I]$ converged to R = 0.05 and R_w = 0.038. The bamfordite crystal structure contains groups of four MoO_6 octahedra, linked by edge-sharing, which in turn are linked through corner-sharing to pairs of FeO_6 octahedra thereby forming infinite sheets parallel to (100). These sheets are stepped and linked by hydrogen bonding. No other molybdenum oxides have this or a similar structure, instead molybdates such as wulfenite, $PbMoO_4$, are based on tetrahedrally coordinated molybdenum.

INTRODUCTION

Despite the widespread occurrence of the sulphide mineral molybdenite, MoS_2, and its susceptibility to weathering processes, there are few common secondary minerals containing essential molybdenum. Existing molybdenum minerals can be subdivided into three groups. (1) Molybdenum oxides such as ferrimolybdite $Fe^{3+}_2(MoO_4)_3 \cdot 8H_2O$, molybdite MoO_3, and sidwillite $MoO_3 \cdot 2H_2O$, which are direct alteration products of molybdenite. (2) Molybdates such as wulfenite $PbMoO_4$, powellite $CaMoO_4$, lindgrenite $Cu_3(MoO_4)_2(OH)_2$, and molybdofornacite $Pb_2Cu[(As,P)O_4][(Mo,Cr)O_4](OH)$, which are formed by the transport of molybdenum in dilute aqueous solutions. (3) U-bearing species such as cousinite $MgU_2Mo_2O_{13} \cdot 6H_2O?$ and iriginite $(UO_2)(Mo_2O_7)$ $\cdot 3H_2O$, which are, in general, poorly characterized and found only in very small amounts.

The new species bamfordite is only the second iron molybdate to be described. It is named for its locality,

Bamford Hill, in northern Queensland, Australia. The mineral data and name were approved by the Commission for New Minerals and Mineral Names before publication. The type specimen is in the Museum of Victoria collection (M7424).

OCCURRENCE

The Bamford Hill W-Mo-Bi deposits are situated about 85 km WSW of Cairns, at latitude 17° 19′ S, longitude 144° 56′ E. Although they were first worked for wolframite in about 1893, the most intense mining activity took place during World War 1. A State Battery operated between 1917 and 1949, but by 1958 the field had been abandoned. The mineralization at Bamford occurred in about 70 quartz pipes distributed in a zone, about 2.5 long and 0.5 km wide, of greisenized granite close to its contact with volcanic rocks (the Featherbed Volcanics; De Keyser and Wolff 1964). The main ore minerals were wolframite, molybdenite, and bismuth, with smaller quan-
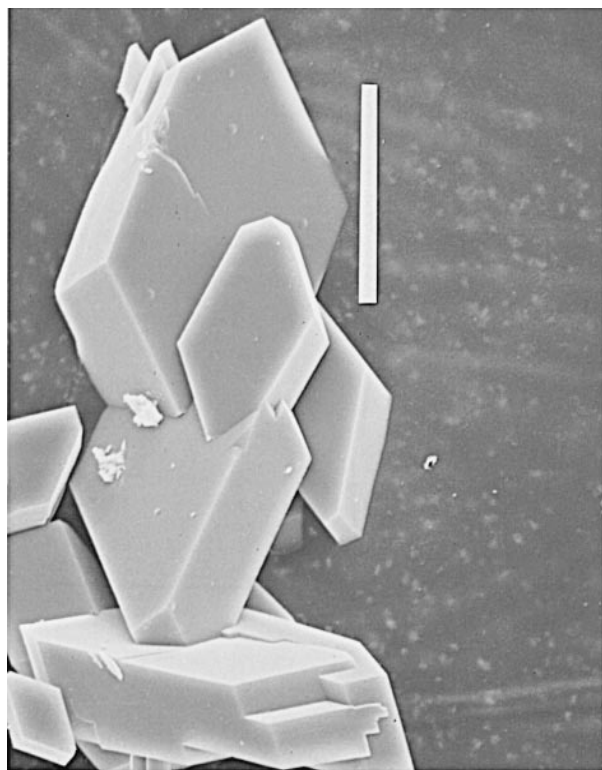
Figure 1. Scanning electron micrograph showing the typical morphology of bamfordite crystals. White scale bar is 20 μm long.

TABLE 1. Chemical analysis of bamfordite

	wt%	No. atoms*
Fe_2O_3	18.93	1.00
MoO_3	68.93	2.01
WO_3	1.90	0.03
P_2O_5	0.39	0.02
H_2O	9.9	4.62
Total	100.05	

* Based on 10 O atoms.

tities of sphalerite, pyrite, chalcopyrite, galena, fluorite, scheelite, powellite, and bismuthinite (Ball 1914). The minerals occurred in miarolitic cavities and vugs, some of which were meters across. These were often filled with clay and fragments of quartz and greisen. According to Ball (1914), the "kaolin" was commonly stained by ochres of tungsten, molybdenum, and bismuth, "often in quantities that should render them marketable." One such ochre, a molybdate of iron, was described by Ball as microcrystalline, submicaceous, and apple-green, with a hardness near three, and a light-green streak. It was found in Grandon's shoot, which was at a depth of about 10 m (Ball 1915) on the Norton's lease. The unknown mineral was later referred to as molybdoferrite by Dunstan (1920).

A small sample from Bamford, fitting the description of Ball's molybdate of iron, was found in the Museum of Victoria collections and partially investigated by one of the authors (W.D.B.) in 1976. An additional specimen was found by E.H. Nickel in the collections of CSIRO Division of Exploration and Mining in Perth, Western Australia, in 1996 and was given to the Museum of Victoria. Enquiries to other museums failed to locate similar material.

APPEARANCE, PHYSICAL, AND OPTICAL PROPERTIES

Bamfordite occurs with small amounts of granular quartz and muscovite as microcrystalline aggregates that vary from compact to friable. Bamfordite grains are individual crystals that are mainly tabular, diamond shaped and 0.005 to 0.05 mm long. Based on triclinic symmetry, the main forms are {001}, {100}, {010}, {110}, and {1$\overline{1}$0} (Fig. 1). The color of the bamfordite aggregates is a strong apple-green with a slight yellowish tinge, resembling fine-grained epidote. The streak is greenish yellow and the hardness between two and three on the Mohs scale. The luster of the aggregates is earthy, but individual crystals are vitreous and transparent under high magnification. Crystals show (100) cleavage traces but no twinning. The density measured by sink-float methods in Clerici solution is 3.620(8) g/cm^3.

The small size of bamfordite crystals and their large refractive indices made accurate determination of optical properties difficult. Crystals are biaxial negative and length slow, with RIs of α = 1.91(1), β = 2.03(1), and γ = 2.11(1), measured using white light. The measured $2V$ is about 90°, in comparison with the 74° calculated. The optical orientation is $\beta \int$ [100], with $c \wedge \gamma'$ = 7°. Crystals show pleochroism from pale to moderate yellowish green.

MAGNETIC PROPERTIES

The Mössbauer spectrum of bamfordite was obtained using a 45 mg sample of finely powdered material on a conventional transmission Mössbauer spectrometer at room temperature (293° K). A single Lorentzian doublet was sufficient to account for all spectral absorption typical of Fe^{2+}. Its hyperfine parameters are 0.387 ± 0.005 mm/s (center shift relative to metallic iron), 0.207 ± 0.005 (quadrupole splitting), and 0.292 ± 0.005 mm/s (linewidth). The center shift indicates that the signal is due to Fe^{3+}. The narrow line width and the low quadrupole splitting suggest that the Fe occupies a single, relatively undistorted octahedral site. Trial fits using an additional doublet with width of 0.29 mm/s and the center shift of 1.14 mm/s, corresponding to Fe^{2+}, indicate that at least 99% of the iron in bamfordite is trivalent.

CHEMICAL COMPOSITION AND X-RAY CRYSTALLOGRAPHY

Six analyses were obtained using a Cameca SX50 microprobe at 15 kV and specimen current of 0.02 μA. Standards were hematite (Fe), pure metals (Mo and W), and fluorapatite (P). No other elements with atomic weights greater than eight were detected in significant

TABLE 2. Powder X-ray diffraction data for bamfordite

I/I_O	d_{obs}	d_{cal}	hkl
30	8.925	8.928	001
10	6.872	6.877	010
30	6.471	6.463	011
70	5.620	5.624	100
10	5.097	5.096	110
8	4.977	4.975	111
12	4.808	4.808	101
	nd	4.797	0$\bar{1}$1
50	4.711	4.711	$\bar{1}$01
3	4.392	4.392	0$\bar{1}$2
70	4.095	4.025	$\bar{1}$11
15	3.864	3.863	$\bar{1}$10
15	3.853	3.852	1$\bar{1}$2
10	3.762	3.761	$\bar{1}$11
3	3.587	3.589	021
25	3.541	3.539	1$\bar{2}$1
15	3.459	3.458	$\bar{1}$02
5	3.377	3.377	120
10	3.363	3.364	1$\bar{1}$1
100	3.319	3.318	0$\bar{1}$2
90	3.232	3.231	022
3	3.211	3.210	122
10	3.015	3.015	$\bar{1}$12
10	2.975	2.976	003
15	2.927	2.928	0$\bar{2}$1
10	2.892	2.893	113
1	2.728	2.723	1$\bar{1}$2
	nd	2.682	023
2	2.678	2.678	123
1	2.656	2.655	103
50	2.614	2.616	212
5	2.545	2.548	$\bar{2}$20
3	2.519	2.518	$\bar{1}$22
7	2.488	2.488	131
10	2.399	2.399	0$\bar{2}$2
	nd	2.385	1$\bar{2}$1
12	2.384	2.383	$\bar{2}$10
9	2.368	2.366	1$\bar{2}$2
15	2.338	2.338	014
7	2.295	2.293	0$\bar{3}$0
1	2.280	2.280	$\bar{2}$12
1	2.228	2.227	133
	nd	2.226	$\bar{1}$23
15	2.154	2.154	033
3	2.091	2.091	1$\bar{0}$4
50	1.956	1.954	$\bar{1}$23
15	1.909	1.910	034
10	1.862	1.863	3$\bar{1}$2
15	1.849	1.849	$\bar{1}$33
5	1.803	1.803	234
7	1.792	1.791	041
10	1.768	1.768	204

TABLE 3. Positional and isotropic equivalent displacement parameters for bamfordite

Atom†	x	y	z	Beq
Mo1	0.2370(1)	0.4809(1)	0.26057(9)	0.47(2)
Mo2	0.0943(2)	0.2340(1)	0.05694(9)	0.59(2)
Fe1	−0.0817(3)	0.8948(2)	0.4069(2)	0.78(3)
O1	−0.216(1)	1.1160(9)	0.5005(7)	0.7(1)
O2*	−0.401(1)	0.925(1)	0.3281(8)	1.4(2)
O3	0.081(1)	0.6791(10)	0.3278(8)	1.1(1)
O4A	0.530(1)	0.4586(9)	0.2840(8)	1.2(1)
O5	0.170(1)	0.2863(10)	0.4072(8)	1.2(1)
O6B	0.338(1)	0.2860(9)	0.1252(7)	0.8(1)
O7C	0.076(1)	0.4876(9)	−0.1364(7)	0.7(1)
O8B	−0.234(1)	0.3275(9)	−0.0392(8)	1.2(1)
O9	−0.017(1)	0.091(1)	0.2212(7)	1.1(1)
O10A	0.244(1)	0.081(1)	−0.0363(8)	1.2(1)

* H_2O.
† See text for designations A, B, C.
‡ Beq = $8/3\pi^2(U_{11}aa^*)^2 + U_{22}(bb^*)^2 + U_{33}(cc^*)^2 + 2U_{11}aa^*bb^*\cos g + 2U_{13}aa^*cc^*\cos b + 2U_{23}bb^*cc^*\cos a$.

sured value (3.620 g/cm³). From unit-cell parameters, $a:b:c = 0.780:1:1.248$.

STRUCTURE DETERMINATION

Experimental methods

A $0.04 \times 0.04 \times 0.06$ mm crystal of the new mineral were isolated from the type specimen for X-ray single crystal structure analysis. Intensity data were measured on a Siemens/Nicolet R3m diffractometer with graphite-monochromated Mo$K\alpha$ radiation. The cell constants and an orientation matrix for the data collection, obtained from a least-squares refinement using the setting angles of 25 carefully centered reflections in the range of $15.60 < 2\theta < 27.90°$, corresponded to a primitive triclinic cell $P1$. The values [$a = 5.878(3)$, $b = 7.536(4)$, $c = 9.436(5)$ Å, $\alpha = 71.66(4)°$, $\beta = 83.43(4)°$, $\gamma = 72.85(4)°$, and $V = 379.0$ Å³] are within experimental error of that obtained by least squares refinement of the powder diffraction pattern. A total of 2348 reflections were collected of which 2221 were unique. An analytical absorption correction was applied to the data, which resulted in transmission factors ranging from 0.78 to 0.85. The data were also corrected for Lorentz and polarization effects.

The structure was solved using direct methods and Fourier techniques. The displacement parameters for the non-H atoms were refined anisotropically. The final cycle of full-matrix least-squares refinement was based on 1486 observed reflections [$I > 2.00 \sigma I$] and 118 variable parameters, and converged to $R = 0.05$, $R_w = 0.038$. Goodness of fit is 1.32. The maximum peak in the final difference map is 1.60 e/A³ and the minimum is −1.94 e/A³. Final atomic coordinates and isotropic equivalent displacement parameters are summarized in Table 3 and anisotropic displacement parameters are given in Table 4, selected bond lengths and angles are in Table 5, a summary of the bond valences of the atoms appears in Table

amounts. The H_2O content was determined separately using a Perkin-Elmer CHN analyzer. The average composition (Table 1) assumes trivalent Fe. Several possible simplified formulae are possible. The final choice, $Fe^{3+}Mo_2O_6(OH)_3 \cdot H_2O$, was based on crystal-structure results (below).

Powder X-ray diffraction data (Table 2) for bamfordite were obtained using a Guinier-Hagg camera with 100 mm diameter, Cr$K\alpha$ radiation, and Si as an internal standard. The data were used to refine a triclinic unit cell with parameters of $a = 5.889(5)$, $b = 7.545(5)$, $c = 9.419(5)$ Å, $\alpha = 71.46(4)°$, $\beta = 83.42(4)°$, $\gamma = 72.78(4)°$, and $V = 378.9(4)$ Å³. The space group is $P1$ or $P\bar{1}$. For $Z = 2$, the calculated density is 3.616 g/cm³, close to the mea-

TABLE 4. Anisotropic displacement parameters for bamfordite

	U_{11}	U_{22}	U_{33}	U_{12}	U_{13}	U_{23}
Mo1	0.0060(4)	0.0057(4)	0.0056(4)	−0.0021(3)	0.0005(3)	−0.0003(3)
Mo2	0.0091(4)	0.0058(4)	0.0068(4)	−0.0031(3)	0.0004(4)	−0.0002(3)
Fe	0.0095(6)	0.0091(7)	0.0098(6)	−0.0027(5)	0.0011(5)	−0.0014(5)
O1	0.006(3)	0.008(3)	0.013(3)	−0.001(3)	−0.002(3)	−0.004(3)
O2	0.014(4)	0.028(4)	0.010(4)	−0.009(3)	−0.002(3)	−0.003(3)
O3	0.022(4)	0.007(3)	0.016(3)	−0.003(3)	0.002(3)	−0.006(3)
O4	0.008(3)	0.013(3)	0.027(4)	−0.005(3)	−0.001(3)	−0.004(3)
O5	0.020(4)	0.010(3)	0.011(4)	−0.007(3)	0.006(3)	0.002(3)
O6	0.012(3)	0.009(3)	0.009(3)	−0.001(3)	0.000(3)	−0.002(3)
O7	0.008(3)	0.007(3)	0.007(3)	−0.002(3)	0.002(3)	0.002(3)
O8	0.017(4)	0.011(3)	0.016(4)	−0.004(3)	−0.002(3)	−0.001(3)
O9	0.011(4)	0.017(4)	0.011(4)	−0.004(3)	0.001(3)	−0.002(3)
O10	0.017(4)	0.015(4)	0.014(4)	−0.001(3)	0.003(3)	−0.009(3)

Note: The general displacement factor expression: $\exp[-2Pi(a^{*2}U_{11}h^2 + b^{*2}U_{22}k^2 + c^{*2}U_{33}l^2 + 2a^*b^*U_{12}hk + 2a^*c^*U_{13}hl + 2b^*c^*U_{23}kl)]$.

6, and a full list of observed and calculated structure factors for the final refinement is supplied in Table 7[1].

Description of structure

In the bamfordite structure, both Fe^{3+} and Mo^{6+} are octahedrally coordinated. Clusters of four MoO_6 edge-sharing octahedra are connected by corners with pairs of FeO_6 edge-sharing octahedra (Fig. 2) to form infinite sheets parallel to (100). These sheets, which are stepped (Fig. 3), are in turn linked by hydrogen bonding. The numbering scheme used is shown in Figure 4. Two crystallographically distinct Mo octahedra exist for which the Mo-O distances give an indication of the distortions present in the octahedra (see Gatehouse and Jozsa 1987). The distances can be correlated with the type of O atom involved, where the O atoms are classified as type A (see Table 3), those with one bond to a molybdenum atom [mean Mo-O 1.69(4) Å]; type B, those with two bonds to Mo [mean Mo-O 1.94(14) Å]; and type C, those with three bonds to Mo [mean Mo-O 2.25(10) Å]. The remaining O atoms are bonded to both Mo and Fe. From Table 5 it is clear that the Mo-O distance increases with increasing sharing of the O atoms between Mo atoms. Where an O atom is shared between a Mo atom and an Fe atom there is remarkable consistency in the Mo-O distance [mean Mo-O 1.772(4) Å]; mean Fe-O distance 1.971(20) Å. The O-Mo-O bond angles vary between 69.2 and 100.7° (see Table 5b). The Fe octahedra are
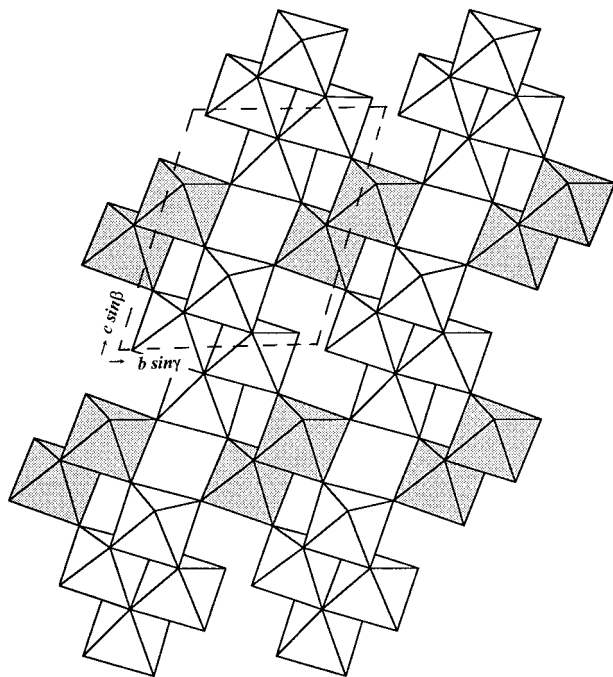
[1] For a copy of Table 7, Document AM-98-003, contact the Business Office of the Mineralogical Society of America (see inside front cover of recent issue) for price information. Deposit items may also be available on the American Mineralogist web site (see inside back cover of a current for web address).

TABLE 5A. Selected bond lengths (Å) for bamfordite

Mo1-O distances		Mo2-O distances		Fe-O distances	
Mo1-O3	1.770(7)	Mo2-O6	1.825(7)	Fe-O1	2.043(7)
Mo1-O4	1.713(7)	Mo2-O7	2.173(6)	Fe-O1	2.013(7)
Mo1-O5	1.776(6)	Mo2-O7	2.355(7)	Fe-O2	2.024(7)
Mo1-O6	2.152(7)	Mo2-O8	2.062(7)	Fe-O3	1.948(7)
Mo1-O7	2.209(7)	Mo2-O9	1.769(7)	Fe-O5	1.979(7)
Mo1-O8	2.132(7)	Mo2-O10	1.657(7)	Fe-O9	1.986(7)

much more regular, with a mean Fe-O distance of 2.00 Å (range 1.948–2.043 Å) and angles ranging from 87.2 to 93.5°. Fe-O bond distances favor Fe^{3+}, in agreement with the interpretation of the Mössbauer spectrum. Calculation of the bond valences for the structure (Table 6) suggests that the O1 atom bonded to Fe is a hydroxyl group and O2 on Fe is an H_2O molecule; these O atoms are only bound to Fe. O7 and O8, both believed to be hydroxyl groups, bridge Mo1 and Mo2. It appears that O4 is hydrogen bonded to the H_2O molecule at O2. Thus

TABLE 5B. Selected bond angles (°) for bamfordite

O3-Mo1-O4	103.6(3)
O3-Mo1-O5	100.0(3)
O3-Mo1-O7	91.3(3)
O3-Mo1-O8	90.4(3)
O4-Mo1-O5	104.5(3)
O4-Mo1-O6	90.9(3)
O4-Mo1-O8	93.1(3)
O5-Mo1-O6	87.5(3)
O5-Mo1-O7	91.1(3)
O6-Mo1-O7	71.3(2)
O6-Mo1-O8	76.9(3)
O7-Mo1-O8	67.7(2)
O9-Mo2-O10	105.7(3)
O8-Mo2-O10	100.7(3)
O8-Mo2-O9	90.7(3)
O6-Mo2-O7	88.9(3)
O6-Mo2-O7	73.7(3)
O6-Mo2-O9	102.9(3)
O6-Mo2-O10	100.8(3)
O7-Mo2-O7	72.2(3)
O7-Mo2-O8	69.6(2)
O7-Mo2-O10	93.3(3)
O7-Mo2-O8	80.1(2)
O7-Mo2-O9	90.0(3)
O1-Fe1-O1	80.7(3)
O1-Fe1-O2	93.0(3)
O1-Fe1-O5	88.9(3)
O1-Fe1-O9	87.9(3)
O1-Fe1-O5	91.2(3)
O1-Fe1-O3	92.8(3)
O1-Fe1-O9	91.4(3)
O2-Fe1-O3	93.5(3)
O2-Fe1-O5	87.2(3)
O2-Fe1-O9	89.8(3)
O3-Fe1-O5	91.0(3)
O3-Fe1-O9	92.5(3)

Note: Estimated standard deviations in the least significant figure are given in parentheses.

TABLE 6. Empirical bond valence sums for the atoms in the refinement of the bamfordite

	Mo1	Mo2	Fe	Sum
O1			0.50 0.46	0.96
O2			0.49	0.49
O3	1.45		0.60	2.05
O4	1.69			1.69
O5	1.42		0.55	1.97
O6	0.51	1.26		1.77
O7	0.44	0.49 0.30		1.23
O8	0.54	0.66		1.20
O9		1.46	0.54	2.00
O10		1.97		1.97
Sum	6.05	6.14	3.14	

FIGURE 3. Structural diagram of bamfordite showing the stepping in the octahedral layers perpendicular to [010]. Shaded octahedra are FeO_6.

FIGURE 2. Structural diagram showing the linkages between MoO_6 octahedra and FeO_6 octahedra (shaded) within the layers which are perpendicular to [100] in bamfordite.

the coordination sphere of Fe is FeO_4OHH_2O and that of Mo is $MoO_4(OH)_2$.

No known molybdenum oxides have this or a similar structure. Possibly, the most closely related Mo mineral is molybdite, MoO_3, which contains MoO_6 linked by corners and edges to form double corrugated layers that, in turn, are held together by weak van der Waals bonds (Povarennykh 1972). The structure of lepidocrocite, FeOOH, also contains double corrugated layers of octahedra, which are linked by hydrogen bonding (Povarennykh 1972). The hexagonal iron molybdenum oxide kamiokite, $Fe_2Mo_3O_8$, has a structure based on alternating layers of MoO_6 and FeO_6 octahedra and FeO_4 tetrahedra (Kanazawa and Sasaki 1986). Sidwillite, $MoO_3 \cdot 2H_2O$, has a structure based on layers of corner-linked MoO_5H_2O octahedra (Cesbron and Ginderow 1985). Other molybdenum oxide minerals, such as ferrimolybdite, $Fe^{3+}_2(MoO_4) \cdot 8H_2O$?, and ilsemannite, $Mo_3O_8 \cdot nH_2O$?, remain structurally undefined.

The molybdate minerals wulfenite, powellite, and lindgrenite all contain Mo in tetrahedral coordination (Povarennykh 1972). It appears that most molybdenum oxysalts formed by direct oxidation of molybdenite contain Mo in octahedral coordination, whereas those which crystallize from transported Mo-bearing fluids, often with large cations such as Pb and Ca, contain tetrahedrally coordinated Mo.

PARAGENESIS

Bamfordite most likely crystallized as a result of supergene alteration of molybdenite in the presence of oxidizing, acidic solutions containing small amounts of tungsten. The timing of the alteration is not known. From the descriptions by Ball (1914), both ilsemannite and ferrimolybdite (a "bright canary yellow,... foliated,. ... subfibrous" iron molybdate collected at the Norton's lease) were among the secondary minerals present. Unfortunately it appears that the variety of ochres noted by Ball have not survived as museum specimens, so that associations of secondary minerals are not available for study.
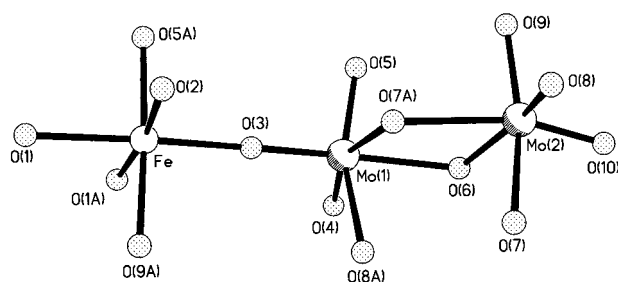
Figure 4. Numbering scheme used for $FeMo_2O_6(OH)_3 \cdot H_2O$. O7A and O8A are $-x, 1 - y, -z$ from O7 and O8; O1A is $-x, 2 - y, 1 - z$ from O1; O5A is $-x, 1 - y, 1 - z$ from O5, and O9 is $x, 1 + y, z$ from O9.

This situation makes it difficult to determine where bamfordite fits in the sequence of alteration, particularly in regard to ferrimolybdite.

From the known hydrolysis equilibria of Mo in dilute solutions, the tetrahedral $(MoO_4)^{2-}$ ion dominates at pH above seven and eight (Baes and Mesmer 1976). With decreasing pH, ionic species such as $(Mo_7O_{24})^{6-}$, based on Mo in octahedral coordination, are more common. This suggests that bamfordite, along with other molybdenum oxysalts with a structure based on linked MoO_6 octahedra, form under more acid conditions than do species with tetrahedrally coordinated Mo. This is consistent with the diminishing acidity expected as Mo-bearing solutions move away from the original sulphide source.

REFERENCES CITED

Baes, C.F. and Mesmer, R.E. (1976) The hydrolysis of cations. Wiley, New York.
Ball, L.C. (1914) The Wolfram, Molybdenite and Bismuth mines of Bamford, North Queensland. Queensland Government Mining Journal, 568–575.
——— (1915) The Wolfram, Molybdenite and Bismuth mines of Bamford, North Queensland. Geological Survey of Queensland, 248, 1–78.
Cesbron, F. and Ginderow, D. (1985) La sidwillite, $MoO_3 \cdot 2H_2O$; une nouvelle espèce minérale de Lake Como, Colorado, USA. Bulletin de Minéralogie, 108, 813–823.
De Kayser, F. and Wolff, K.W. (1964) The geology and mineral resources of the Chillagoe area. Geological Survey of Queensland, 317.
Dunstan, B. (1920) Queensland Industrial Minerals. Review of occurrences, treatment, uses, values and production: IV. Molybdenum. Queensland Government Mining Journal, vol. XXL, no. 246, 462–466.
Gatehouse, B.M. and Jozsa, A.J. (1987) The crystal structure of potassium dimolybdate hydrate. Journal of Solid State Chemistry, 71, 34–39.
Kanazawa, Y. and Sasaki, A. (1986) Structure of kamiokite. Acta Crystallographica, C42, 9–11.
Povarennykh, A.S. (1972) Crystal chemical classification of minerals, 766 p. Plenum Press, New York.